Supporting Information

Triple Bonding Between Beryllium and Nitrogen in HNBeCO

Lina Wang[1,4], Sudip Pan[2,4], Guanjun Wang[1], Xiaoqing Zeng[1], Mingfei Zhou[1,*] & Gernot Frenking[2,3,*]

[1] Department of Chemistry, Shanghai Key Laboratory of Molecular Catalysts and Innovative Materials, Fudan University, Shanghai 200438, China.

[2] Fachbereich Chemie, Philipps-Universität Marburg, Hans-Meerwein-Strasse 4, D-35043 Marburg, Germany.

[3] Institute of Advanced Synthesis, School of Chemistry and Molecular Engineering, Nanjing Tech University, Nanjing 211816, China

[4] These authors contributed equally: Lina Wang, Sudip Pan

* Corresponding Authors: mfzhou@fudan.edu.cn; frenking@chemie.uni-marburg.de

Table of Contents

Methods

Experimental methods. The 1064 nm fundamental of a Nd:YAG laser (Continuum, Minilite II, 10 Hz repetition rate and 6 ns pulse width) was used to ablate a rotating bulk beryllium target to produce beryllium atoms. The laser-evaporated beryllium atoms were co-deposited with HNCO in excess neon onto a cryogenic CsI window, which was maintained at 4 K by means of a closed-cycle helium refrigerator. The HNCO/Ne mixtures were prepared in a stainless-steel vacuum line using a standard manometric technique. After 30 min of sample deposition at 4 K, IR absorption spectra in the mid-infrared region (4000–450 cm^{-1}) were recorded with a Bruker Vertex 80V spectrometer at a 0.5 cm^{-1} resolution using a liquid nitrogen cooled broad band HgCdTe (MCT) detector. Bare mirror backgrounds, recorded prior to sample deposition were used as references in processing the sample spectra. The spectra were subjected to baseline correction to compensate for infrared light scattering and interference patterns. Samples were annealed to the desired temperatures and cooled back to 4 K for spectral acquisition. For selected samples, photo-excitations were performed through a quartz window mounted on the assembly.

Isocyanic acid HNCO was prepared according to literature[1] by heating a mixture of stearic acid (0.57 g, 2 mmol) and sodium cyanate (0.13 g, 2 mmol) at 90 °C in a glass vessel (25 ml), which was connected to the dynamic vacuum line (0.1 pa) through a poly(tetrafluoroethylene) Young-valve. All the volatile products were condensed in a liquid nitrogen trap and then purified by fractional distillation through three successive cold U-traps at −80, −135, and −196 °C. Pure isocyanic acid was retained in the middle trap, and its quality was checked by gas-phase IR spectroscopy (Bruker, Tensor 27). Isotopically-labeled samples $HN^{13}CO$ and $H^{15}NCO$ were prepared using the ^{13}C and ^{15}N-labeled potassium cyanates.[2] For the synthesis of ^{15}N-labeled sodium cyanate, a 25-mL flame-dried round bottom flask containing 1.32 g (10 mmol) of potassium phenoxide was added with 2 mL of 4-methyl-2-pentanol, which has been dried over 3Å molecular sieves. Then 0.62 g (10 mmol) of ^{15}N-labeled urea was added as a solid, and the reaction was heated and stirred at 135 °C under nitrogen for 2 hours. As the reaction

proceeds, an off-white precipitate begins to form. The reaction was then cooled to ambient temperature, and the precipitate was filtered and washed with three portions of cold ethanol (2 mL). The solid was then dried under high vacuum, affording 0.62 g (7.6 mmol) ^{15}N-labeled potassium cyanate. The ^{13}C-labeled potassium cyanate was prepared using the ^{13}C-labeled urea with the same method.

Theoretical Methods. The geometry optimization and vibrational spectra elucidation of HNBeCO and the fragments were calculated at the CCSD(T)-Full[3,4]/def2-TZVPP and M06-2X-D3[5]/def2-TZVPP levels of theory. The partial charges following the original Hirshfeld suggestion[26] were calculated using the CCSD(T)-Full/def2-TZVPP optimized geometry. The calculated vibrational frequencies at CCSD(T)-Full/def2-TZVPP are scaled by 0.956 as suggested in the literature.[6] Time-dependent TD-DFT[7,8] B3LYP/6-311+G(3df) calculations were performed for the calculation of UV-Vis transitions. All these calculations were carried out with Gaussian 16.[9] The NBO calculations were carried out with the version 6.0.[10]

The bonding situation in HNBeCO complex was further analyzed by means of an energy decomposition analysis (EDA)[11] together with the natural orbitals for chemical valence (NOCV)[12,13] method by using the ADF 2018.105 program package.[14,15] The EDA-NOCV calculations[16,17] were carried out at the M06-2X/TZ2P level using the M06-2X-D3/def2-TZVPP optimized geometry. TZ2P is a triple-ζ quality basis set augmented by two sets of polarization functions.[18] In this analysis, the intrinsic interaction energy (ΔE_{int}) between two fragments can be divided into three energy components as follows:

$$\Delta E_{\text{int}} = \Delta E_{\text{elstat}} + \Delta E_{\text{Pauli}} + \Delta E_{\text{orb}} \qquad (1)$$

The electrostatic ΔE_{elstat} term represents the quasiclassical electrostatic interaction between the unperturbed charge distributions of the prepared fragments, the Pauli repulsion ΔE_{Pauli} corresponds to the energy change associated with the transformation from the superposition of the unperturbed electron densities of the isolated fragments to the wavefunction, which properly obeys the Pauli principle through explicit antisymmetrization and renormalization of the production wavefunction. The orbital

term ΔE_{orb} is originated from the mixing of orbitals, charge transfer and polarization between the isolated fragments, which can be further decomposed into contributions from each irreducible representation of the point group of the interacting system as follows:

$$\Delta E_{orb} = \sum_{r} \Delta E_{r} \qquad (2)$$

The combination of the EDA with NOCV enables the partition of the total orbital interactions into pairwise contributions of the orbital interactions which is very vital to get a complete picture of the bonding. The charge deformation $\Delta\rho_k(r)$, resulting from the mixing of the orbital pairs $\psi_k(r)$ and $\psi_{-k}(r)$ of the interacting fragments presents the amount and the shape of the charge flow due to the orbital interactions (Equation 3), and the associated energy term ΔE_{orb} provides with the size of stabilizing orbital energy originated from such interaction (Equation 4).

$$\Delta\rho_{orb}(r) = \sum_{k} \Delta\rho_k(r) = \sum_{k=1}^{N/2} \nu_k [-\psi_{-k}^2(r) + \psi_k^2(r)] \quad (3)$$

$$\Delta E_{orb} = \sum_{k} \Delta E_k^{orb} = \sum_{k=1}^{N/2} \nu_k [-F_{-k,-k}^{TS} + F_{k,k}^{TS}] \qquad (4)$$

More details about the EDA-NOCV method and its application are given in recent review articles.[19-25]

References

(1) Drozdoski, W. S.; Baronavski, A. P.; McDonald, J. R. Photodissociation of HNCO at 193 nm. NH($a^1\Delta$) Internal Energy Distribution and Reaction Rate with O_2. *Chem. Phys. Lett.* **1979,** *64*, 421-425.

(2) Filer, C. N.; Peng, C. T. An Alternative and Simple Synthesis of [(14)C]potassium Cyanate. *J. Label. Compd. Radiopharm.* **2020,** *63*, 240-242.

(3) Purvis III, G. D.; Bartlett, R. J. A Full Coupled-cluster Singles and Doubles Model: The Inclusion of Disconnected Triples. *J. Chem. Phys.* **1982**, *76*, 1910-1918.

(4) Pople, J. A.; Head-Gordon, M.; Raghavachari, K. Quadratic Configuration Interaction. A General Technique for Determining Electron Correlation Energies. *J. Chem. Phys.* **1987**, *87*, 5968-5975.

(5) Zhao, Y.; Truhlar D. G. The M06 Suite of Density Functionals for Main Group Thermochemistry, Thermochemical Kinetics, Noncovalent Interactions, Excited States, and Transition Elements: Two New Functionals and Systematic Testing of Four M06-class Functionals and 12 Other Functionals. *Theor Chem Acc.* **2008**, *120*, 215-241.

(6) Computational Chemistry Comparison and Benchmark Data Base (CCCBDB), National Institute of Standards and Technology (NIST), Release 21, August 2020, https://cccbdb.nist.gov/vibscalejust.asp.

(7) Stratmann, R. E.; Scuseria, G. E.; Frisch, M. J. An Efficient Implementation of Time-dependent Density-functional Theory for the Calculation of Excitation Energies of Large Molecules. *J. Chem. Phy.* **1998,** *109*, 8218-8224.

(8) Foresman, J. B.; Head-Gordon, M.; Pople, J. A.; Frisch, M. J. Toward a Systematic Molecular Orbital Theory for Excited States. *J. Phys. Chem.* **1992,** *96*, 135-149.

(9) Frisch, M. J., et al. Gaussian 16. Gaussian A.03, Inc. Wallingford, CT. **2016**.

(10) Glendening, E. D.; Landis, C. R.; Weinhold, F. NBO 6.0: Natural Bond Orbital Analysis Program. *J. Comput. Chem.* **2013,** *34*, 1429-1437.

(11) Ziegler, T.; Rauk, A. On the Calculation of Bonding Energies by the Hartree Fock Slater Method. *Theoret. Chim. Acta* **1977**, *46*, 1-10.

(12) Mitoraj, M.; Michalak, A. Donor–acceptor Properties of Ligands from the

Natural Orbitals for Chemical Valence. *Organometallics* **2007**, *26*, 6576-6580.

(13) Mitoraj, M.; Michalak, A. Applications of Natural Orbitals for Chemical Valence in a Description of Bonding in Conjugated Molecules. *J. Mol. Model.* **2008**, *14*, 681-687.

(14) ADF2018, SCM, Theoretical Chemistry, Vrije Universiteit, Amsterdam, The Netherlands, http://www.scm.com.

(15) te Velde, G.; Bickelhaupt, F. M.; Baerends, E. J.; Fonseca Guerra, C.; van Gisbergen, S. J. A.; Snijders, J. G.; Ziegler, T. Chemistry with ADF. *J. Comput. Chem.* **2001,** *22*, 931-967.

(16) Michalak, A.; Mitoraj, M.; Ziegler, T. Bond Orbitals from Chemical Valence Theory. *J. Phys. Chem. A* **2008,** *112*, 1933-1939.

(17) Mitoraj, M. P.; Michalak, A.; Ziegler, T. A Combined Charge and Energy Decomposition Scheme for Bond Analysis. *J. Chem. Theory Comput.* **2009,** *5*, 962-975.

(18) Van Lenthe, E.; Baerends, E. J. Optimized Slater-Type Basis Sets for the Elements 1–118. *J. Comput. Chem.* **2003,** *24*, 1142-1156.

(19) Zhao, L.; von Hopffgarten, M.; Andrada, D. M.; Frenking, G. Energy Decomposition Analysis. *WIREs Comput. Mol. Sci.* **2018,** *8*, e1345.

(20) Frenking, G.; Bickelhaupt, F. M. in *The Chemical Bond. Fundamental Aspects of Chemical Bonding*, Frenking, G. and Shaik (Eds), S. S, Wiley-VCH, Weinheim, **2014**, 121-158.

(21) Frenking, G.; Tonner, R.; Klein, S.; Takagi, N.; Shimizu, T.; Krapp, A.; Pandey, K. K.; Parameswaran, P. New Bonding Modes of Carbon and Heavier Group 14 Atoms Si–Pb. *Chem. Soc. Rev.* **2014,** *43*, 5106-5139.

(22) Zhao, L.; Hermann, M.; Holzmann, N.; Frenking, G. Dative Bonding in Main Group Compounds. *Coord. Chem. Rev.* **2017,** *344*, 163-204.

(23) Frenking, G.; Hermann, M.; Andrada, D. M.; Holzmann, N. Donor–acceptor Bonding in Novel Low-coordinated Compounds of Boron and Group-14 Atoms C–Sn. *Chem. Soc. Rev.* **2016,** *45*, 1129-1144.

(24) Zhao, L.; Hermann, M.; Schwarz, W. H. E.; Frenking, G. The Lewis Electron-pair Bonding Model: Modern Energy Decomposition Analysis. *Nat. Rev. Chem.* **2019,** *3*, 48-63.

(25) Zhao, L.; Pan, S.; Holzmann, N.; Schwerdtfeger, P.; Frenking, G. Chemical Bonding and Bonding Models of Main-group Compounds. *Chem. Rev.* **2019,** *119*, 8781-8845.

(26) Hirshfeld, E.L. *Theor. Chim. Acta* **1977**, *44*, 129.

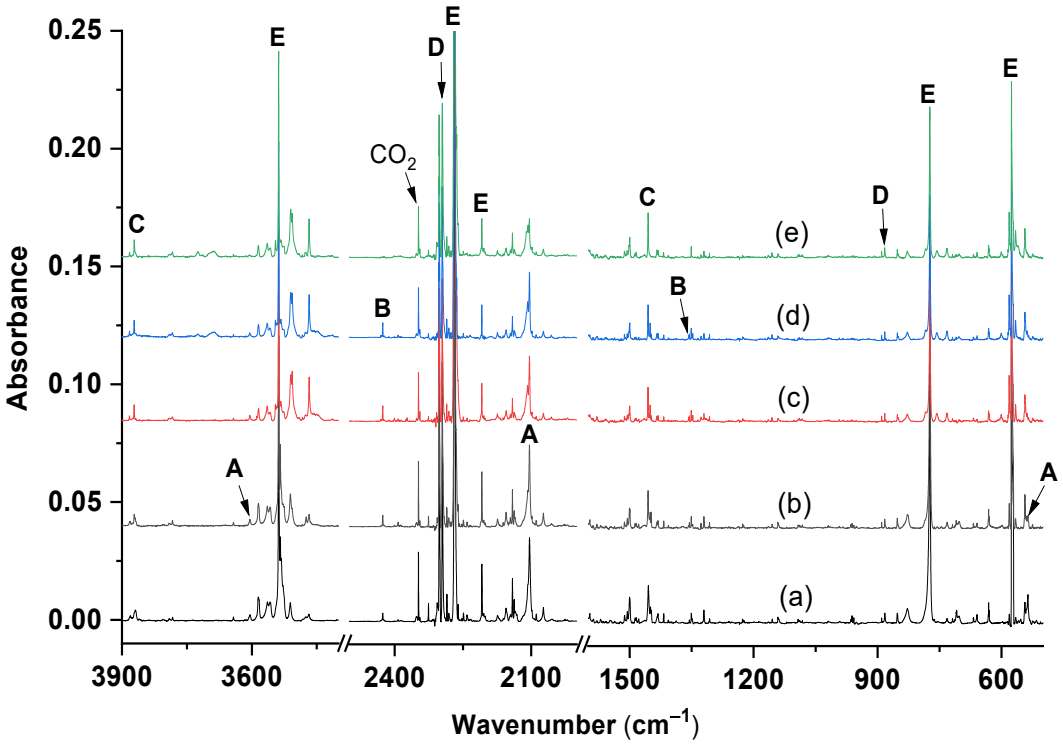

Figure S1. Infrared (IR) spectra in the 3900−3400, 2500−2000 and 1600−500 cm^{-1} regions from co-deposition of laser-ablated beryllium atoms with 0.025% HNCO in neon. (a) 30 min of sample deposition at 4 K, (b) 10 K annealing, (c) 12 K annealing, (d) 5 min of blue light (440 nm) irradiation, and (e) 5 min of 280 nm light irradiation. **A**: HNBeCO, **B**: $BeOCNH^+$, **C**: HOBeCN, **D**: BeNCO, and **E**: HNCO.

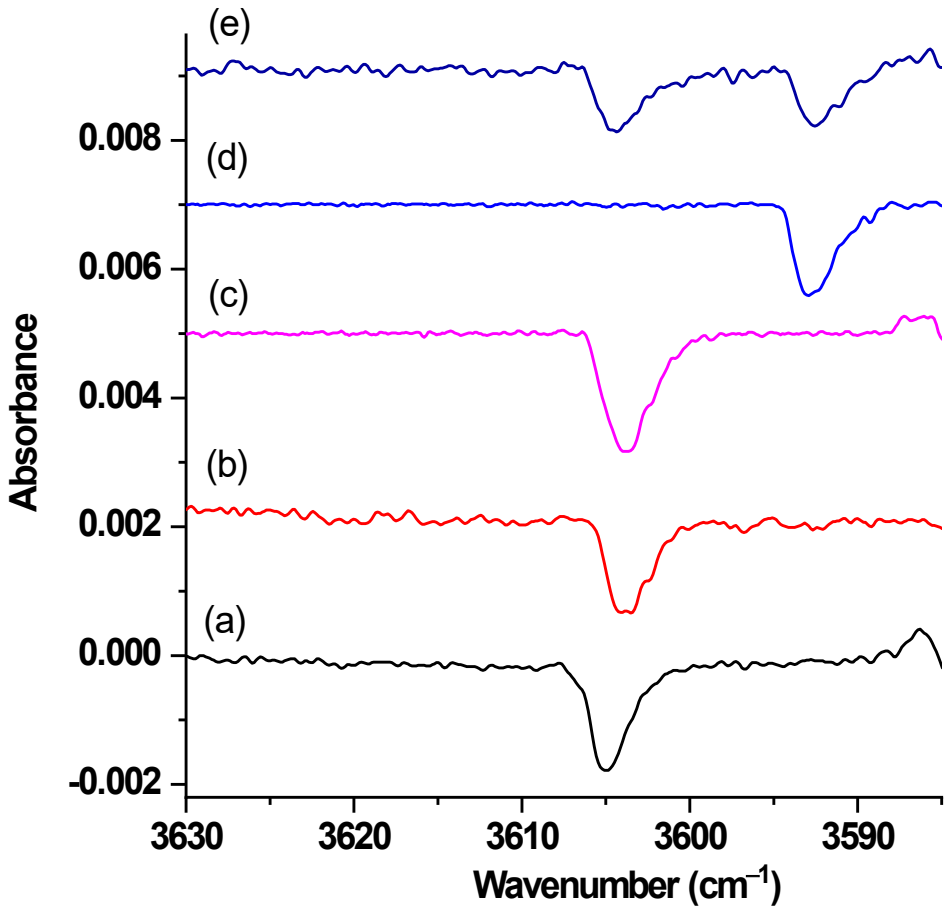

Figure S2. IR difference spectra in the 3630−3585 cm^{-1} region from co-deposition of laser-ablated beryllium atoms with 0.05% HNCO in neon. (Spectra taken after 5 min of 280 nm light irradiation minus the spectrum taken after 5 min of blue light (440 nm) irradiation). (a) 0.05% $H^{14}N^{12}CO$, (b) 0.05% $H^{14}N^{13}CO$, (c) 0.05% $H^{14}N^{12}CO$ + 0.05% $H^{14}N^{13}CO$, (d) 0.05% $H^{15}N^{12}CO$, and (e) 0.05% $H^{14}N^{12}CO$ + 0.05% $H^{15}N^{12}CO$.

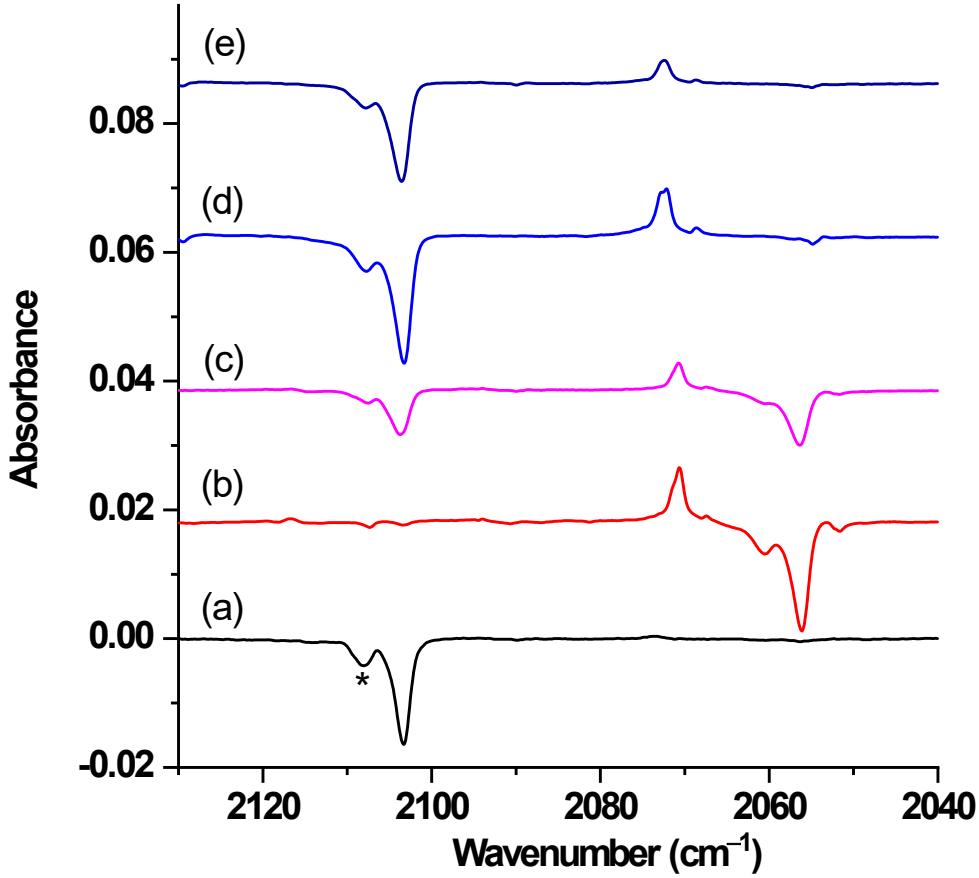

Figure S3. IR difference spectra in the 2130−2040 cm^{-1} region from co-deposition of laser-ablated beryllium atoms with 0.05% HNCO in neon. (Spectra taken after 5 min of 280 nm light irradiation minus the spectrum taken after 5 min of blue light (440 nm) irradiation). (a) 0.05% $H^{14}N^{12}CO$, (b) 0.05% $H^{14}N^{13}CO$, (c) 0.05% $H^{14}N^{12}CO$ + 0.05% $H^{14}N^{13}CO$, (d) 0.05% $H^{15}N^{12}CO$, and (e) 0.05% $H^{14}N^{12}CO$ + 0.05% $H^{15}N^{12}CO$. The band labeled with * is due to a site absorption.

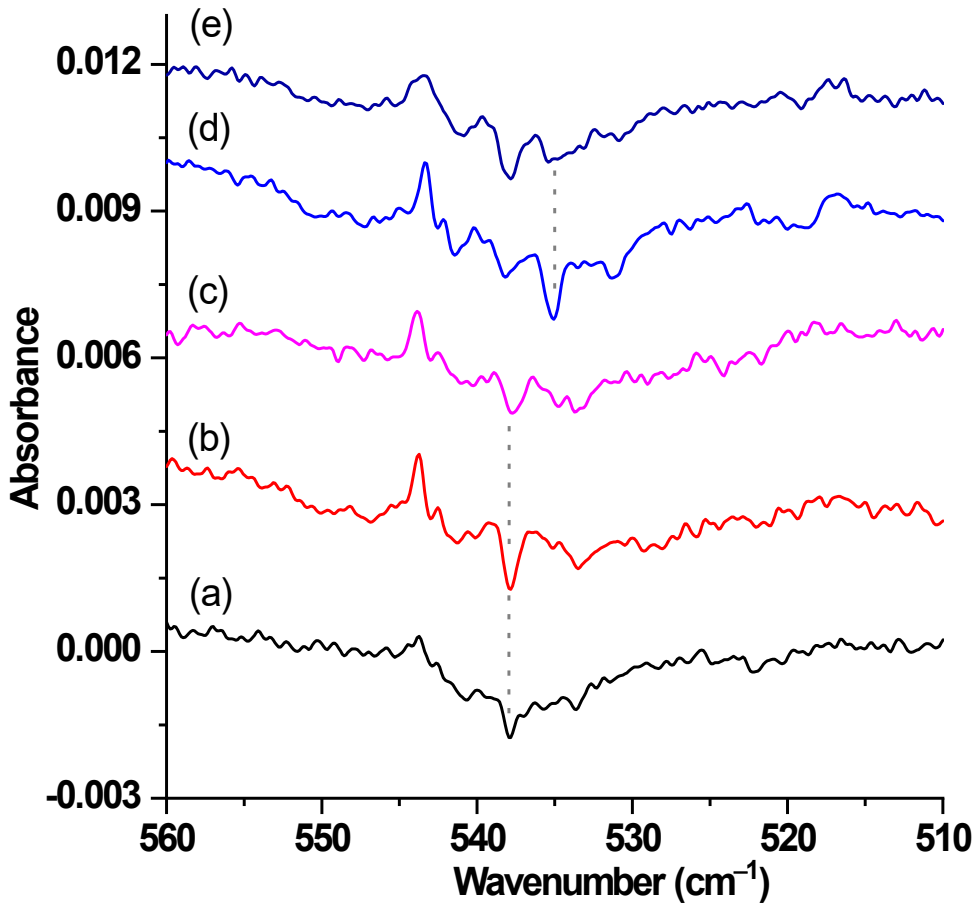

Figure S4. IR difference spectra in the 560−510 cm^{-1} region from co-deposition of laser-ablated beryllium atoms with 0.05% HNCO in neon. (Spectra taken after 5 min of 280 nm light irradiation minus the spectrum taken after 5 min of blue light (440 nm) irradiation). (a) 0.05% $H^{14}N^{12}CO$, (b) 0.05% $H^{14}N^{13}CO$, (c) 0.05% $H^{14}N^{12}CO$ + 0.05% $H^{14}N^{13}CO$, (d) 0.05% $H^{15}N^{12}CO$, and (e) 0.05% $H^{14}N^{12}CO$ + 0.05% $H^{15}N^{12}CO$.

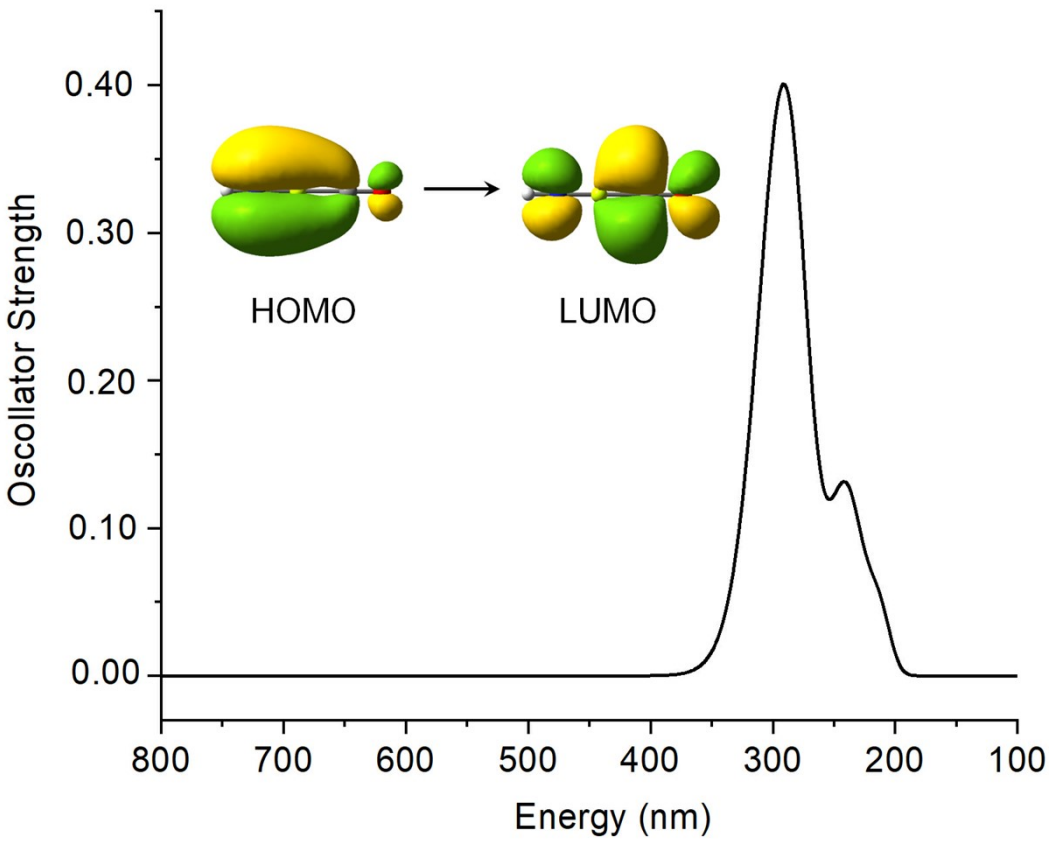

Figure S5. Computed ultraviolet-visible (UV/Vis) absorption spectrum of HNBeCO at the TD-B3LYP/6-311+G(3df) level. The calculated strong absorption band (λ_{max} = 291 nm) corresponds to the HOMO→LUMO transition.

Table S1. The EDA-NOCV results using NH and BeCO with different charges and electronic states as interacting fragments at the M06-2X/TZ2P//M06-2X-D3/def2-TZVPP level.

Energy	HN ($X^3\Sigma^-$, $3\sigma^2 1\pi^2$) + BeCO ($^3\Sigma^-$, $6\sigma^2 3\pi^2$)	HN ($^3\Pi$, $3\sigma^1 1\pi^3$) + BeCO ($X^3\Pi$, $7\sigma^1 3\pi^1$)	HN ($^1\Sigma^+$, $2\sigma^2 1\pi^4$) + BeCO ($^1\Sigma^+$, $7\sigma^2 3\pi^0$)	HN^- ($X^2\Pi$, $3\sigma^1 1\pi^4$) + $BeCO^+$ ($X^2\Sigma^+$, $7\sigma^1 3\pi^0$)	HN^{2-} ($X^1\Sigma^+$, $3\sigma^2 1\pi^4$) + $BeCO^{2+}$ ($X^1\Sigma^+$, $7\sigma^0 3\pi^0$)
ΔE_{int}	−176.4	−221.0	−383.3	−386.3	−851.3
$\Delta E_{\mathrm{Pauli}}$	49.0	183.0	218.4	157.6	120.1
$\Delta E_{\mathrm{Metahybrid}}$	16.5	19.1	17.2	17.3	10.6
$\Delta E_{\mathrm{elstat}}$	−41.1	−98.8	−84.7	−254.8	−752.1
ΔE_{orb}	−200.8	−324.3	−534.3	−306.4	−230.0

Table S2. Calculated vibrational frequencies (cm^{-1}) and IR intensities ($km\ mol^{-1}$) of OCBeNH at the M06-2X-D3/def2-TZVPP and CCSD(T)-Full/def2-TZVPP levels.

Mode	ν(M06-2X)	ν(CCSD(T))	I(M06-2X)
C-Be-N bending	44.4	33.9	13
	44.4	33.9	13
Be-C-O bending	427.0	422.6	5
	427.0	422.6	5
Be-C stretching	473.5	490.4	29
Be-N-B bending	596.2	560.1	66
	596.2	560.1	66
Be-N stretching	1606.1	1483.1	0
C-O stretching	2315.1	2155.3	760
N-N stretching	3788.4	3749.9	84

Table S3. The Cartesian coordinates of HNBeCO, HN and BeCO at the CCSD(T)-Full/def2-TZVPP level.

HNBeCO			
E = −183.1661742 au			
0 1			
O	0.000000000	0.000000000	2.031858000
C	0.000000000	0.000000000	0.900847000
Be	0.000000000	0.000000000	−0.793976000
N	0.000000000	0.000000000	−2.185604000
H	0.000000000	0.000000000	−3.184810000
HN			
E = −55.1609161 au			
0 3			
N	0.000000000	0.000000000	0.129708000
H	0.000000000	0.000000000	−0.907953000
BeCO			
E = −127.8121737 au			
0 3			
O	0.000000000	0.000000000	1.015372000
C	0.000000000	0.000000000	−0.143808000
Be	0.000000000	0.000000000	−1.815032000